Electronic Supplementary Information

Hydrogen bond-directed supramolecular polymorphism leading to soft and hard molecular ordering

Takumi Aizawa,[a] Keisuke Aratsu,[a] Sougata Datta,[b] Takaki Mashimo,[c] Tomohiro Seki,[c]
Takashi Kajitani,[d] Fabien Silly[e] and Shiki Yagai*[b,f]

[a]*Division of Advanced Science and Engineering, Graduate School of Science and Engineering, Chiba University, 1-33 Yayoi-cho, Inage-ku, Chiba 263-85223, Japan.*

[b] *Department of Applied Chemistry and Biotechnology, Graduate School of Engineering, Chiba University, 1-33 Yayoi-cho, Inage-ku, Chiba 263-8522, Japan.*

[c]*Division of Applied Chemistry and Frontier Chemistry Center (FCC) Faculty of Engineering, Hokkaido University Kita 13 Nishi 8 Kita-ku, Sapporo, Hokkaido 060-8628, Japan.*

[d]*Suzukakedai Materials Analysis Division, Technical Department, Tokyo Institute of Technology, 4259 Nagatsuta, Midori-ku, Yokohama 226-8503, Japan.*

[e]*TITANS, SPEC, CEA, CNRS, Université Paris-Saclay, CEA Saclay, F-91191 Gif sur Yvette, France*

[f]*Institute for Global Prominent Research (IGPR), Chiba University, 1-33 Yayoi-cho, Inage-ku, Chiba 263-8522, Japan.*

E-mail: yagai@faculty.chiba-u.jp

Table of Contents

1. Materials and Methods

Column chromatography was performed using 63–210 µm silica gel. All commercially available reagents and solvents were of reagent grade and used without purification. The solvents for the preparation of the assemblies were all spectral grade and used without purification. ^{1}H and ^{13}C NMR spectra were recorded on JEOL JNM-ECA500 NMR spectrometer and chemical shifts are reported in perts per million (ppm, δ) with the signal of tetramethylsilane (TMS) as the internal standard. ESI-MS spectra were measured on an Exactive (Thermo Scientific). UV/vis spectra were recorded on a JASCO V660 spectrophotometer with Peltier device temperature-control unit. Fluorescence spectra were measured with JASCO FP-8300 with a JASCO ETC-815 temperature controller using a screw capped quartz cuvette with optical path length of 1.0 cm. AFM images were acquired under ambient conditions using a Multimode 8 Nanoscope V microscope (Bruker Instruments) in peak force tapping (Scanasyst) mode. Silicon cantilevers (SCANASYST-AIR) with a spring constant of 0.4 N/m and frequency of 70 kHz (nominal value, Bruker, Japan) were used. Samples were prepared by spin-coating solutions onto freshly cleaved HOPG at 3000 rpm for 1 min, 10 µL. FT-IR spectra were measured on JASCO FT / IR-4600 spectrometer. STM images were acquired 1-Phenyloctane (98%, Aldrich) solutions of the compounds were prepared at different concentrations. A droplet of these solutions was then deposited on a graphite substrate. STM imaging of the samples was performed at the liquid–solid interface using a Pico-SPM (Molecular Imaging, Agilent Technology) scanning tunneling microscope. Cut Pt/Ir tips were used to obtain constant current images at room temperature with a bias voltage applied to the sample. STM images were processed and analyzed using the application FabViewer. 2. The emission quantum yields of solution sample of **TF** and **PN** were recorded on a Hamamatsu Quantaurus-QY spectrometer with an integrating sphere. Optical and Polarized optical microscopic observation was carried out using an Olympus BX51 optical microscopy system with a Linkam temperature-controlled heating stage. DSC was performed on SII DSC6220.

Synchrotron X-ray diffraction analysis of liquid crystalline 2: X-ray diffraction (XRD) patterns of bulk sample were measured using the BL45XU beamline at SPring-8 (Hyogo, Japan) equipped with a Pilatus3X 2M (Dectris) detector. The scattering vector ($q = 4\pi\sin\theta/\lambda$) and the position of the incident X-ray beam on the detectors were calibrated using several orders of layer reflections from silver behenate (d = 58.380 Å), where 2θ and λ refer to the scattering angle and wavelength of the X-ray beam (1.0 Å), respectively. The sample-to-detector distance was 0.4 m. The obtained diffraction patterns were integrated along the Debye–Scherrer ring to afford 1D intensity data using FIT2D software.[S1]

Powder X-ray diffraction analysis of plate-like nanostructures of PN: Powder XRD patterns of bulk sample were measured using 0.154 nm X-ray (CuKα-beam) in the transparent mode using NANO-Viewer (Rigaku Corp.) equipped with a Pilatus 100K (Dectris) detector. The scattering angle (2θ) and the position of the incident X-ray beam on the detectors were calibrated using several orders of layer reflections from silver behenate (d = 58.380 Å). The sample-to-detector distance was 7 cm. The obtained diffraction patterns were integrated along the Debye–Scherrer ring to afford 1D intensity data using 2DP software (Rigaku Corp.).

X-ray structural analyses: Single-crystal X-ray structural analyses were carried out on a Rigaku XtaLAB PRO MM007 diffractometer using graphite monochromated Cu-Kα radiation. The structure was solved by direct methods and expanded using Fourier techniques. Non-hydrogen atoms were refined anisotropically. Hydrogen atoms were refined using the riding model. All calculations were performed using the Olex2 crystallographic software package except for refinement, which was performed using SHELXL-2018.[S2] Simulated powder patterns were generated with Mercury 4.1[S3] from the structures determined by the single-crystal diffraction analyses.

2. Synthesis and Characterization.

Synthesis of compound **2** was reported previously.[S4] Compound **3** for X-ray crystallography was synthesized according to Scheme S1.

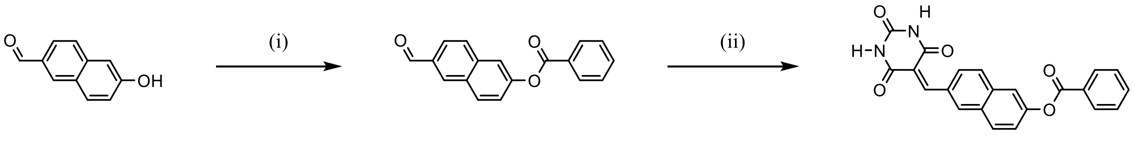

4 **3**

Scheme S1. Synthesis of **3**. (i) DCC, DMAP, THF, rt; (ii) barbituric acid, EtOH, reflux.

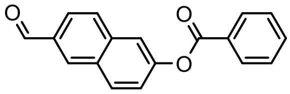

Synthesis of compound 4: 6-hydroxy-2-naphthaldehyde (1.05 g, 5.81 mmol), benzoic acid (2.29 g, 17.4 mmol), *N*,*N*-dimethyl-4-aminopyridine (DMAP, 93 mg, 0.6 mmol) and dicyclohexylcarbodiimide (DCC, 1.4 g, 11.7 mmol) were dissolved in dry THF (15 mL). The mixture was stirred for 24 h at room temperature under N_2 atmosphere. After the resulting white precipitates were filtered off, the filtrate was diluted with AcOEt and washed with water and brine. The organic layer separated was dried over Na_2SO_4 and then evaporated to dryness under a reduced pressure. The resulting solid was purified by column chromatography over silica gel (AcOEt:Hexane = 1:4) to give **4** as white solids (1.5 g, 91% yield). ^{1}H NMR (500 MHz, DMSO-d_6, 293 K): δ 10.17 (s, 1H), 8.63 (s, 1H), 8.26 (d, J = 8.98 Hz, 1H), 8.17 (dd, J = 1.3, 8.34 Hz ,2H), 8.07 (d, J = 8.52 Hz, 1H), 7.97 (d, J = 2.25 Hz, 1H), 7.96 (dd, J = 1.65, 8.52 Hz, 1H), 7.79 (tt, J = 2.58, 14.92 Hz, 1H), 7,63-7.60 (m, 3H). ^{13}C NMR (125 MHz, DMSO-d_6, 293 K): δ 193.41, 165.12, 157.12, 151.32, 137.08, 134.84, 134.33, 131.91, 130.45, 129.62, 129.26, 129.22, 123.75, 123.60, 119.78. HRMS (ESI): *m/z* calcd for $C_{18}H_{13}O_3$ 277.0859 $[M+H]^+$, found 277.0856.

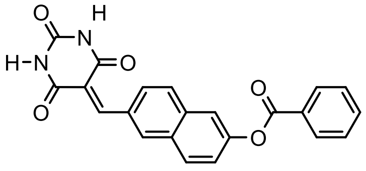

Synthesis of compound 3: 4 (1.0 g, 0.603 mmol) and barbituric acid (1.85 g, 14.5 mmol) in EtOH (100 mL) was stirred for 12 h at 75 °C under reflux. The reaction mixture was cooled to room temperature and the resulting precipitates were collected by filtration and washed with hot ethanol repeatedly to give pure compound **3** as yellow solids (1.2 g, 85% yield). ^{1}H NMR (500 MHz, DMSO-d_6, 293 K): δ 11.4 (s, 1H), 11.26 (s,1H), 8.68 (s, 1H), 8.42 (s,1H), 8.21 (dd, J = 8.8 Hz, 1H), 8.17 (dd, J = 1.34, 8.37 Hz ,2H), 8.08 (d, J = 9.1 Hz, 1H), 7.94 (d, J = 8.8 Hz, 1H), 7.89 (d, J = 2.2 Hz, 1H), 7.75 (tt, J = 2.6, 14.9 Hz, 1H), 7.61 (t, J = 15.6 Hz, 2H), 7.54 (dd, J = 2.3, 8.9 Hz, 2H). ^{13}C NMR (125 MHz, DMSO-d_6, 293 K); δ 165.15, 163.94, 164.21, 154.88, 150.92, 150.81, 135.53, 135.45, 134.79, 131.53, 131.00, 130.69, 130.43 129.91, 129.60, 129.27, 127.40, 123.04, 119.73, 119.32. HRMS (APCI): *m/z* calcd for $C_{22}H_{15}O_5N_2$ 387.0975 $[M+H]^+$, found 387.0985.

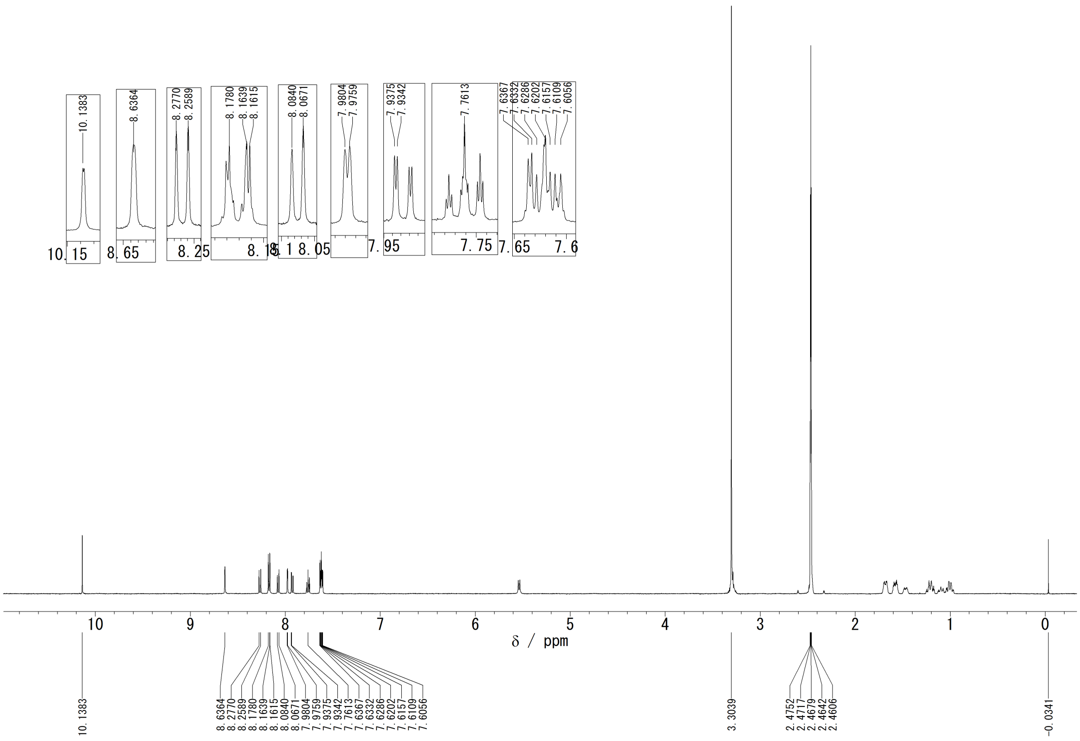

Chart S1. ^{1}H NMR spectrum of compound **4** in DMSO-d_6 at 293 K.

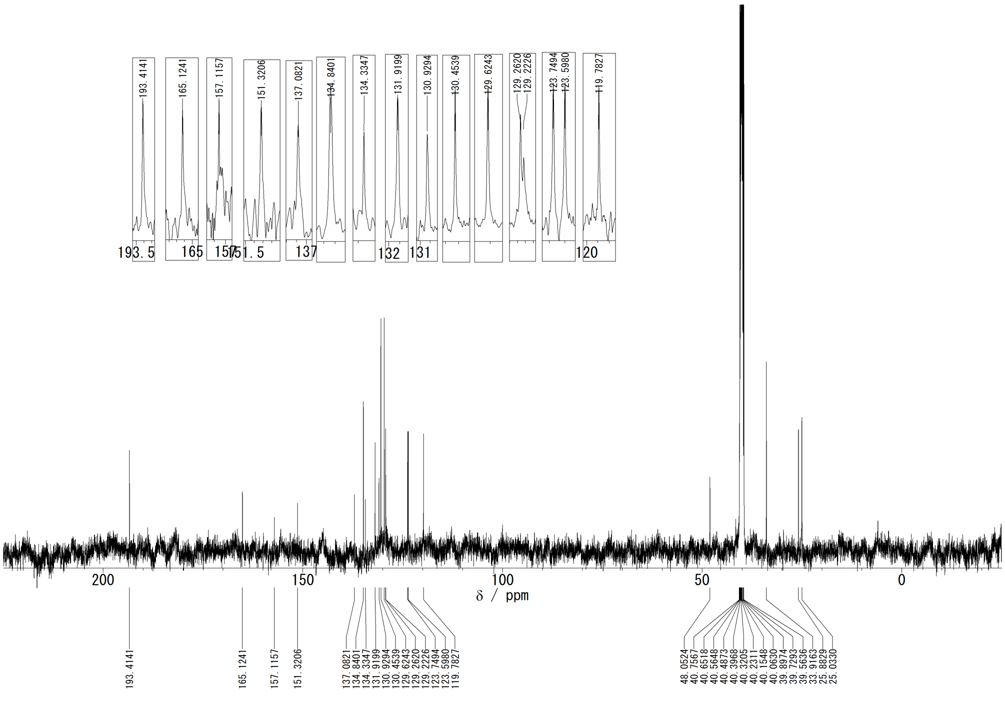

Chart S2. ^{13}C NMR spectrum of compound **4** in DMSO-d_6 at 293 K.

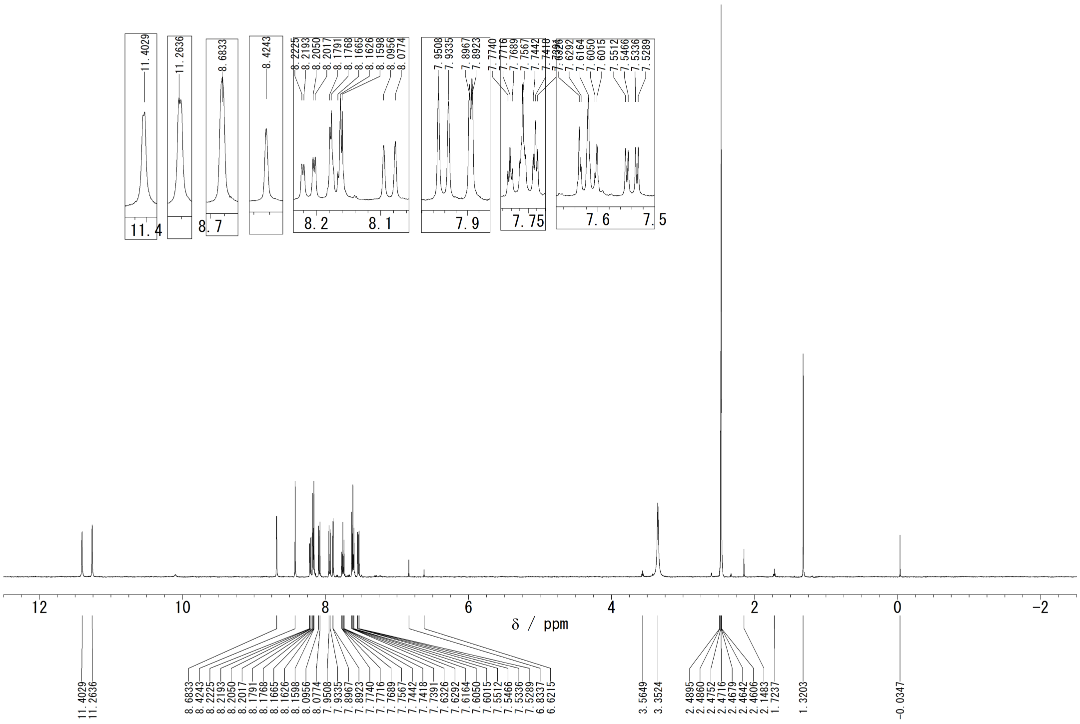

Chart S3. ^{1}H NMR spectrum of compound **3** in DMSO-d_6 at 293 K.

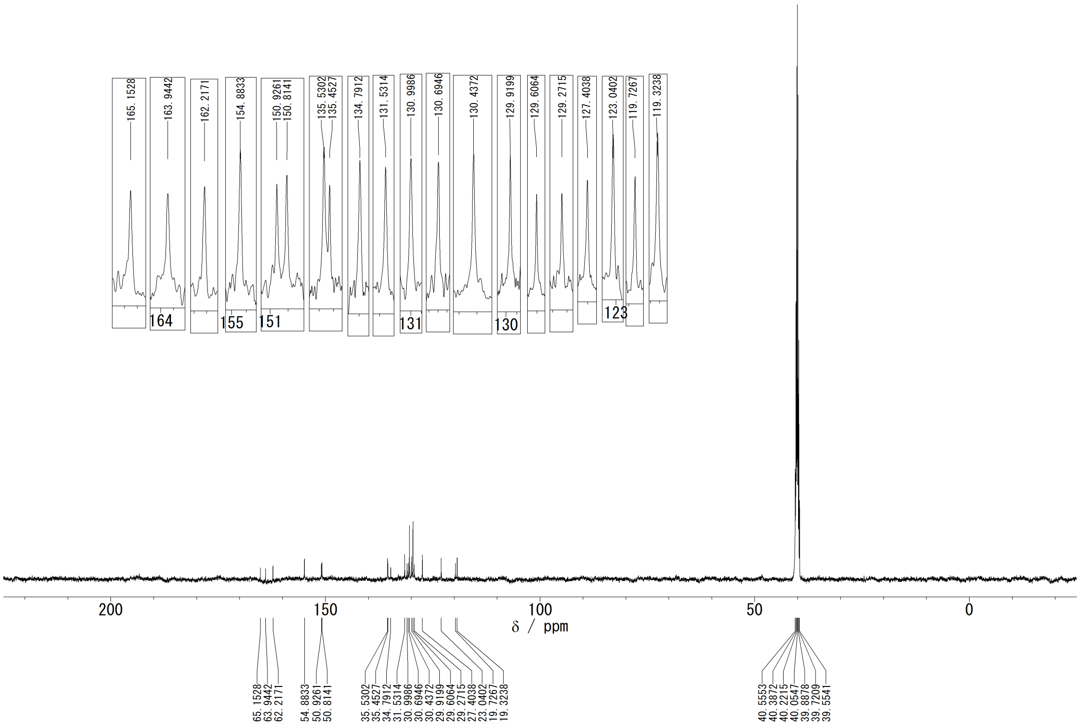

Chart S4. ^{13}C NMR spectrum of compound **3** in DMSO-d_6 at 293 K.

3. Supporting Figures

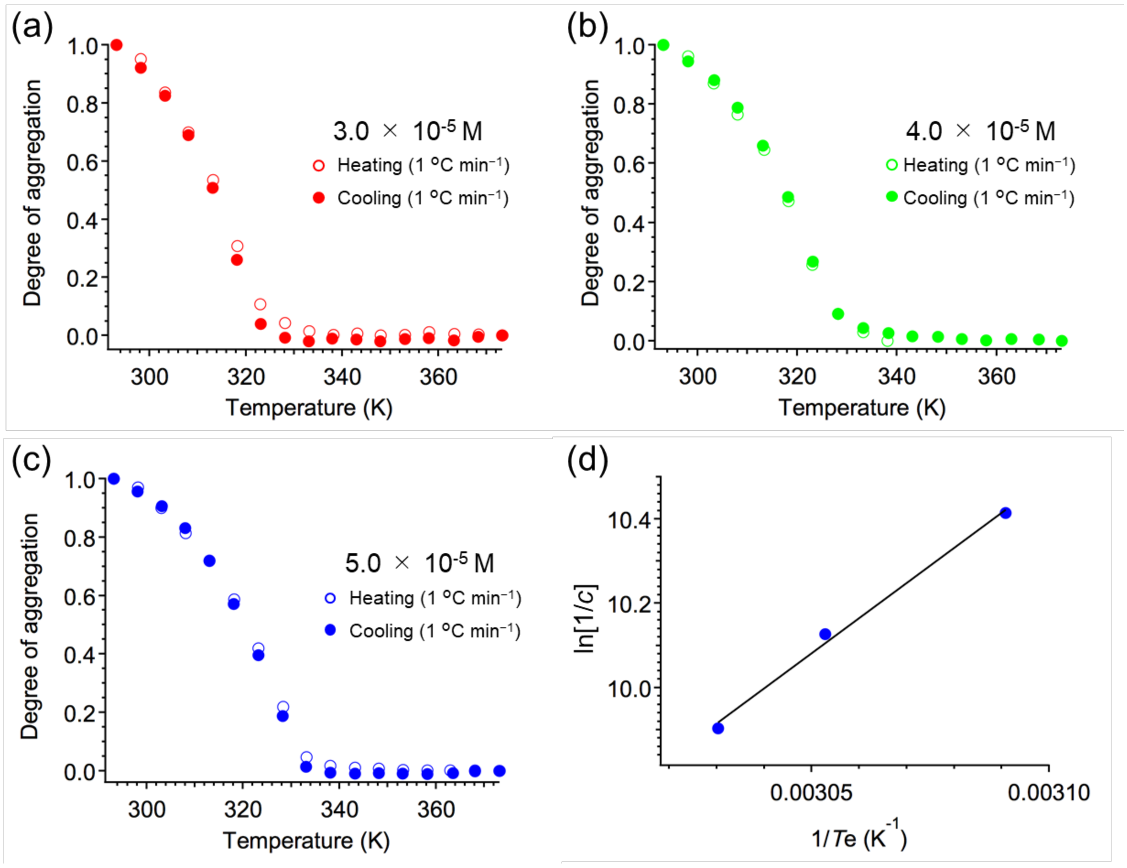

Fig. S1 (a−c) Degree of aggregation of **2** as a function of temperature during cooling and heating MCH solutions at a rate of 1 °Cmin^{-1}, which were estimated from the UV−Vis absorption spectral changes measured at (a) $c = 3.0 \times 10^{-5}$ M, (b) 4.0×10^{-5} M and (c) 5.0×10^{-5} M. (d) van't Hoff plot of the natural logarithm of the reciprocal concentration as a function of the reciprocal temperature ($1/T_e$). The black line shows the corresponding linear fit. The thermodynamic parameters were evaluated from this plot: $\Delta H° = -58$ kJ mol^{-1}, $\Delta S° = -92$ J mol^{-1} K^{-1}, $\Delta G° = -31$ kJ mol^{-1} at 293 K.

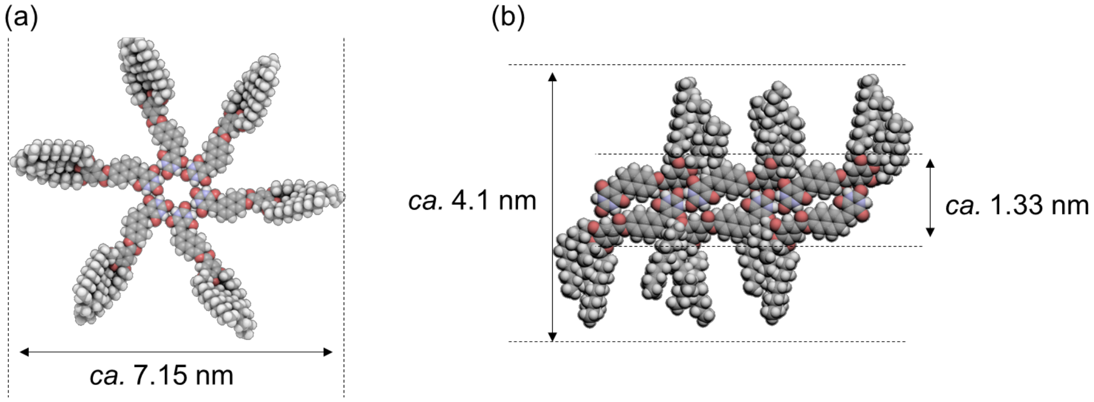

Fig. S2 Geometry-optimized structures of (a) hydrogen-bonded hexameric rosette of **2** and (b) ester-mediated hydrogen-bonded supramolecular array of **2**. These structures were calculated by AMBER force field without solvent using MacroModel 10.4.

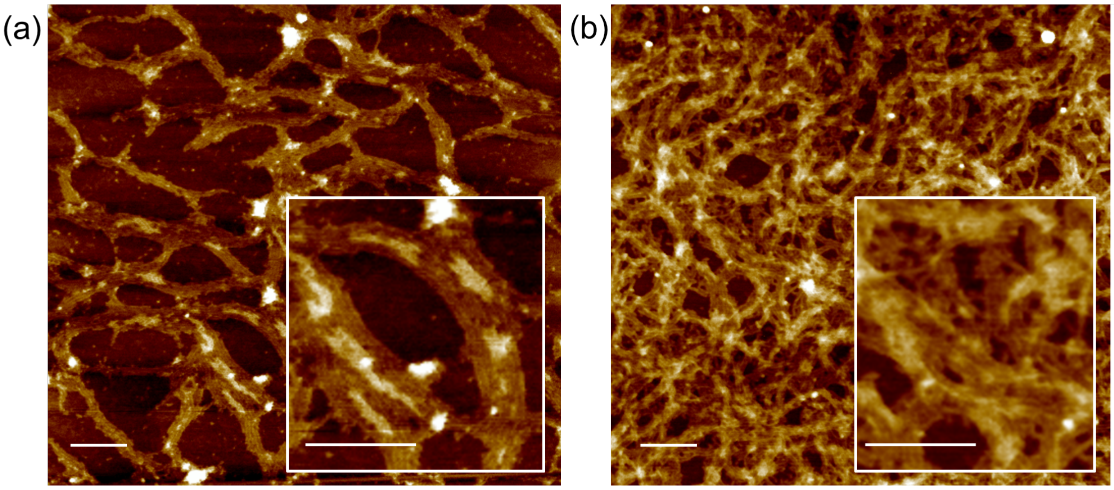

Fig. S3 Additional AFM images of **TF** spin-coated immediately after cooling MCH solutions of **2** at $c = 2.5 \times 10^{-4}$ M (a) and $c = 5.0 \times 10^{-4}$ M (b). Insets are magnified images. Scale bars = 100 nm.

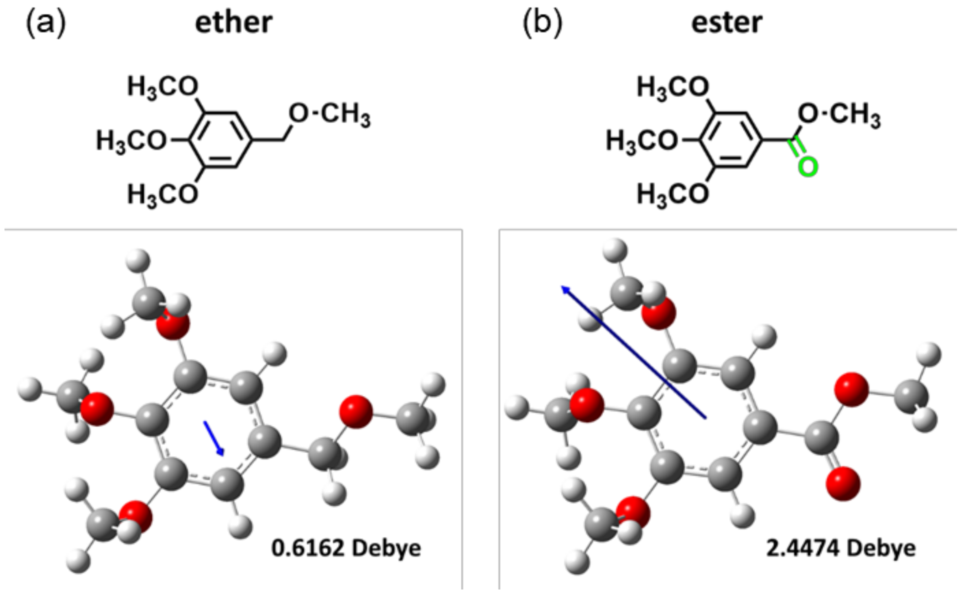

Fig. S4 Calculated electric dipole moment of (a) 1,2,3-trimethoxy-5-(methoxymethyl)benzene and (b) methyl 3,4,5-trimethoxybenzoate (B3LYP/6-31 G(d,p)).

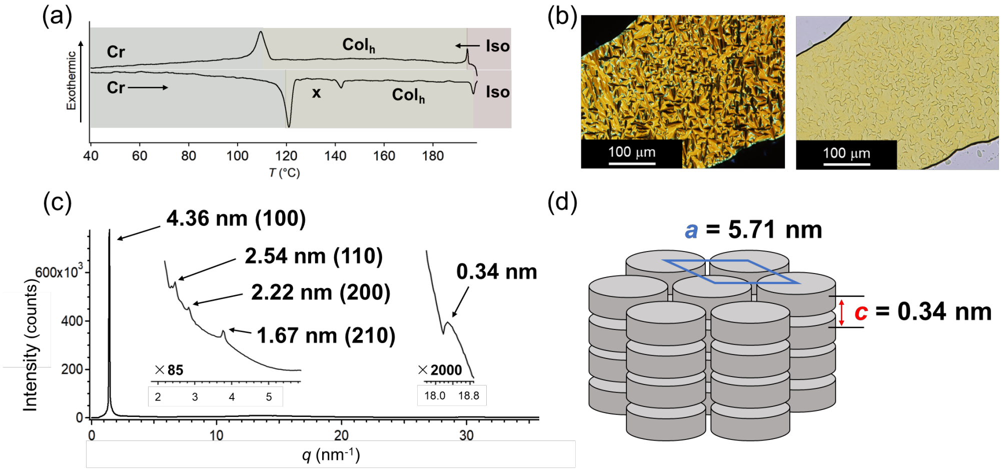

(e) $Z = (\rho VN)/M$

$$=((1.0\ \mathrm{g\ /\ cm^{-3}})\times(5.71\times10^{-7}\mathrm{cm})^{2}\times(0.343\times10^{-7}\mathrm{cm})\times(\sin120°)\times(6.02\times10^{23}\ \mathrm{/mol}))\ /\ (939.332\ \mathrm{g/mol})$$

$$=6.20$$

Fig. S5 (a) DSC thermograms of **2** upon heating from 30 to 195 °C (below) and subsequent cooling the resulting isotropic melt from 195 to 30 °C (upper) at scan rate of 3 °C min^{-1}. The initial sample was prepared by cooling the isotropic melt. (b) POM (left) and optical microscopy images (right) at 170 °C. (c) Synchrotron X-ray diffraction patterns of bulk sample of **2** at 170 °C. (d) Schematic representation of the $\mathrm{Col_h}$ structure of **2**. (e) Calculation of *Z* value.

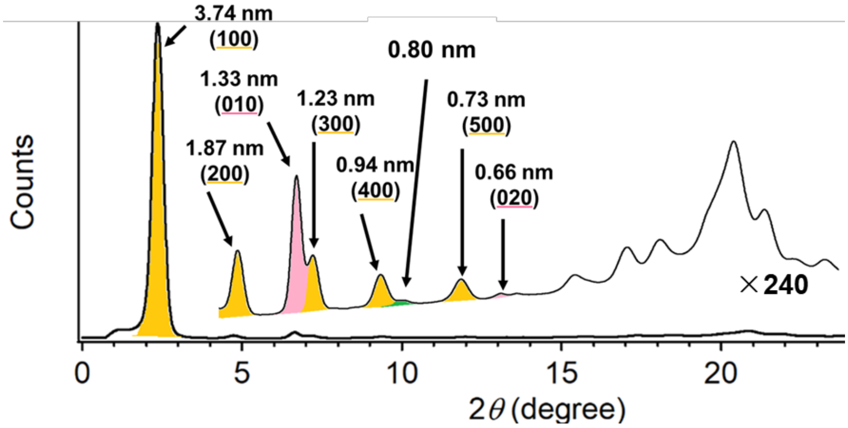

Fig. S6 Powder XRD pattern of bulk sample of **PN** obtained by aging a MCH solution of **2** ($c = 1.0 \times 10^{-2}$ M) at r.t.

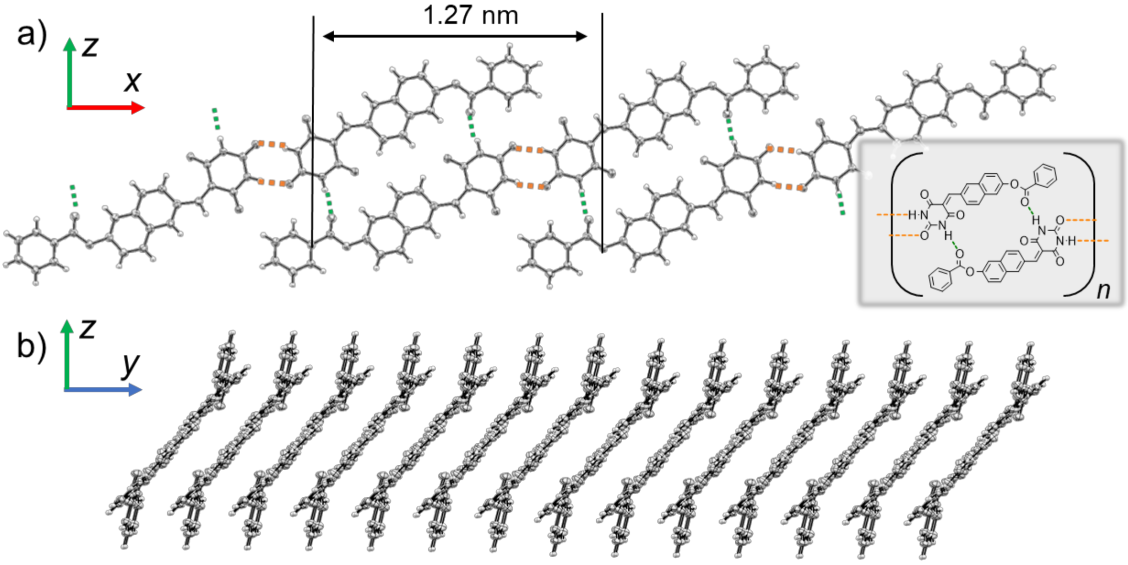

Fig. S7 (a,b) Single-crystal structure of **3** along (a) *x* axis (hydrogen-bonding direction) and (b) *y* axis (stacking direction of the hydrogen-bonded chain). Green dotted lines show H-bonding between NH of barbituric acid and C=O of ester group. Orange dotted lines show hydrogen bonds between the other NH and a C=O of two barbituric acid units.

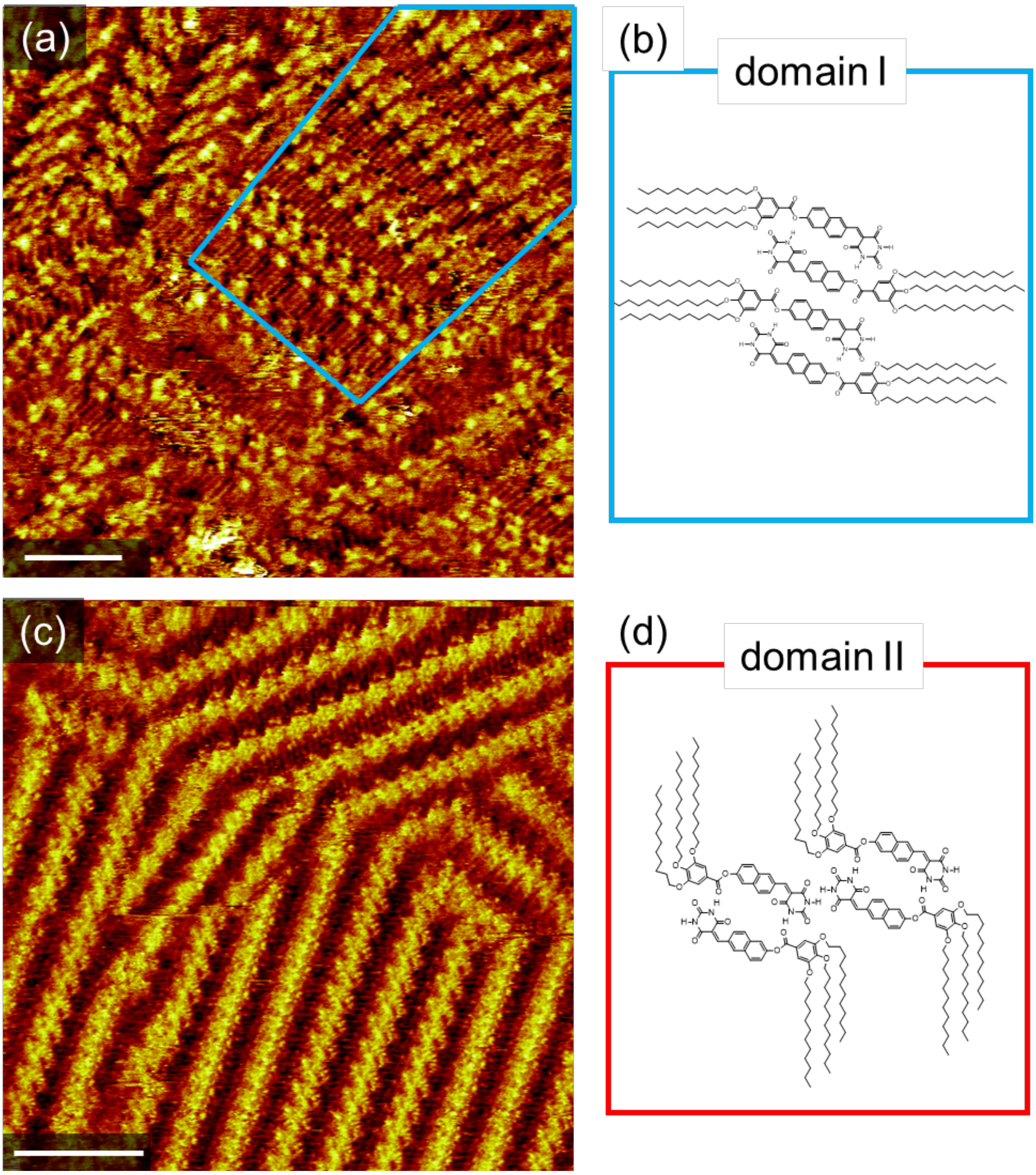

Fig. S8 (a,c) STM images and (b,d) the corresponding structural models of two different molecular packing (domain I, a and b; domain II, c and d) of **2** at the 1-phenyloctane/HOPG interface. $V_s = 1.3$ V, $I_t = 9$ pA. Concentration: 1.0×10^{-2} M. Scale bars = 5 nm.

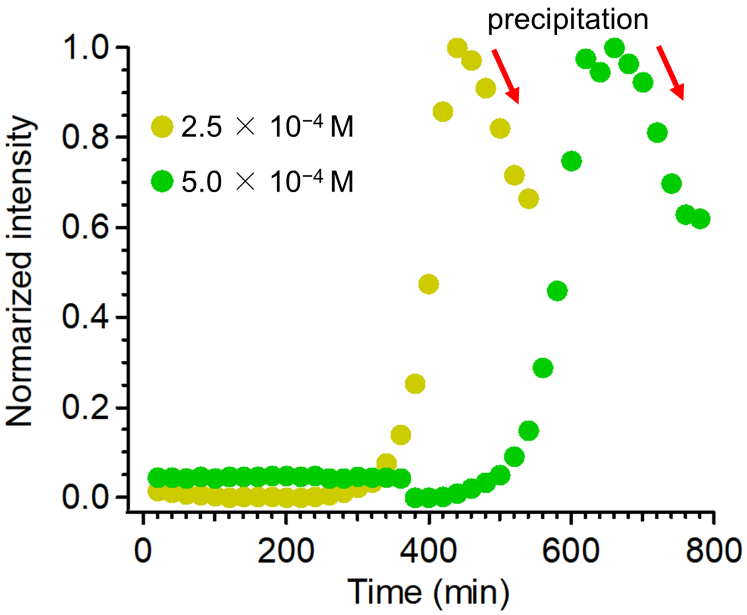

Fig. S9 Plots of normalized fluorescence intensity at 650 nm (λ_{ex} = 346 nm) upon aging a MCH solution of **2** with different concentrations (yellow dots, $c = 2.5 \times 10^{-4}$ M; green dots, $c = 5.0 \times 10^{-4}$ M) at 30 °C after cooling from 100 to 20 °C at a rate of 1 °C min^{-1}. Red arrows indicate a decrease in fluorescence intensity due to precipitation.

4. Data for Single-Crystal X-ray Structural Analysis

Table S1. Summary of X-ray crystallographic data for **3**.

Compound	**3**
CCDC number	1980882
Empirical Formula	$C_{22}H_{14}N_2O_5$
Formula Weight	386.35
Crystal Size / mm	0.2×0.03×0.02
Crystal System	monoclinic
a / Å	12.79790(10)
b / Å	5.74316(5)
c / Å	22.89076(19)
α / °	90
β / °	92.3207(7)
γ / °	90
V / Å^3	1681.10(2)
Space Group	$P2_1/n$
Z value	4
D_{calc} / g cm^{-3}	1.527
Temperature / K	123
$2\theta_{\mathrm{max}}$ / °	153.448
μ (Cu $K\alpha$) / mm^{-1}	0.917
No. of Reflection	Total: 27058
	Unique: 3405
	$R_{\mathrm{int}} = 0.0332$
R_1 (all data)	0.0461
R_1 ($I \geq 2\sigma(I)$)	0.0419
wR_2 (all data)	0.1169
wR_2 (I $\geq 2\sigma(I)$)	0.1140
Goodness of Fit	1.065
Max./Mini. Peak I / Å	0.33 e^- / −0.26 e^-

5. Supporting References

S1. http://www.esrf.eu/computing/scientific/FIT2D/

S2. G. M. Sheldrick, *Acta Cryst. Sect. C*, 2015, **71**, 3−8.

S3. https://www.ccdc.cam.ac.uk/support-and-resources/Downloads/

S4. K. Aratsu, S. Yagai et al., *unpublished data.*